



# Green synthesis and microcalorimetric study of a novel *N*-alkylation Schiff base and its bismuth(III) complex

Xu Li<sup>1</sup> · Ge-Yan Le<sup>1</sup> · Qiang-Guo Li<sup>1</sup> · Jian-Hong Jiang<sup>1</sup> · Fan-hua Zeng<sup>1</sup> · Xia Li<sup>1</sup> · Chuan-Hua Li<sup>1</sup>

Received: 1 July 2020 / Accepted: 29 March 2021 / Published online: 13 April 2021  
© Akadémiai Kiadó, Budapest, Hungary 2021

## Abstract

A new *N*-alkylation Schiff base [*N*<sup>2</sup>,*N*<sup>6</sup>-bis(2-hydroxy-3-methoxybenzyl)pyridine-2,6-dicarboxamide] was synthesized from *o*-vanillin and pyridine-2,6-dicarboxamide by a solid-phase microwave green synthesis without catalyst and solvent. A new bismuth(III) complex was prepared by reaction of the ligand with BiCl<sub>3</sub>. The ligand and its bismuth(III) complex were characterized by elemental analysis, spectral techniques (<sup>1</sup>HNMR, MS, FT-IR and UV), chemical analysis, thermogravimetric analysis and molar conductance. The compositions of the ligand and its bismuth(III) complex were (C<sub>23</sub>H<sub>23</sub>N<sub>3</sub>O<sub>6</sub>) and Bi(C<sub>23</sub>H<sub>21</sub>N<sub>3</sub>O<sub>6</sub>)Cl. Moreover, the antibacterial activity of the ligand and its bismuth(III) complex against *S. pombe* was evaluated by bio-microcalorimetry at 32 °C. The quantitative relationship between some thermokinetic parameters (*k*, *t*<sub>G</sub> and *I*) with the concentration (*c*) of the ligand and its bismuth(III) complex was investigated. The half inhibition concentrations (*IC*<sub>50</sub>) of the ligand and its bismuth(III) complex were obtained as 4.63 × 10<sup>-3</sup> mol dm<sup>-3</sup> and 2.10 × 10<sup>-3</sup> mol dm<sup>-3</sup>, respectively. The results showed that the antibacterial activity of bismuth(III) complex was stronger than that of the ligand. Further, the action target of bismuth(III) complex on bovine serum albumin (BSA) was studied by the molecular docking simulation method, and we found that bismuth(III) complex bounded at in the hydrophobic cavity of the substructure domain IIB of BSA.

**Keywords** *O*-Vanillin · Pyridine-2,6-dicarboxamide · Bismuth(III) complex · Solid-phase microwave green synthesis · Bio-microcalorimetry

## Introduction

*o*-Vanillin and its Schiff base compounds have strong antibacterial activities [1–3]. Compounds containing pyridine groups [4] and amides containing aromatic ring substituents have both better antibacterial activities [5], such as pyridine-2,6-dicarboxamide compounds, and their derivatives have also good antibacterial effect [6]. Bismuth is the only green heavy metal element in nature with relative cheap, low toxicity and low radioactivity. Organic bismuth compounds have been widely used in the field of medicine [7–11]. For

example, bismuth subcitrate, bismuth salicylate, ranitidine bismuth citrate and other drugs, with antisecretory, cell protection and anti-*Helicobacter pylori*, are used to treat gastric and duodenal ulcers [12, 13]. In recent years, exploring the antibacterial and antitumor activity of organic bismuth compounds has become a research hot spot [14–17].

*Schizosaccharomyces pombe* (*S. pombe*) has become an ideal model organism for studying eukaryotic cells, because *S. pombe* have obvious mitotic cycle, similar to the human cell division process, and playing an important role in studying the mechanism of action of drugs [18]. The biological analysis of microcalorimetry is based on release of heat in cell metabolism. Various metabolic processes in living cells are accompanied by energy transfer and change of heat. The inhibition of cell metabolism by microcalorimetry is based on the interaction between inhibitors and cells, which changes the heat of cells production. The decrease in cell heat production reflects the inhibition of various biochemical reactions in the process of cellular metabolism. The increase in cell heat production reflects the vigorous process of cell metabolism,

✉ Qiang-Guo Li  
liqiangguo@163.com

✉ Chuan-Hua Li  
lichuanhua0526@126.com

<sup>1</sup> Hunan Provincial Key Laboratory of Xiangnan Rare-Precious Metals Compounds and Applications, College of Chemical Biology and Environmental Engineering, Xiangnan University, Chenzhou 423043, Hunan Province, People's Republic of China

which is beneficial to the growth of cell metabolism. It has been proved that microcalorimetry may be the best way to measure cell metabolism because it reflects the sum of cellular metabolic processes and can directly determine the different sensitivity of various cells to their inhibitors [19, 20]. Microcalorimetry is a general, real-time, non-damage and highly sensitive method based on biothermokinetics. It has been gradually applied in the assay of biological activity in vitro. This method has significant advantages over traditional assay methods such as continuous dilution method and agar plate diffusion method [21, 22].

In this work, a new *N*-alkylation Schiff base was directly reacted by *o*-vanillin with electron-deficient pyridine-2,6-dicarboxamide using a novel solid-phase microwave green synthesis method, which required neither catalyst nor solvent. A new bismuth(III) complex was synthesized reacting of the ligand and BiCl<sub>3</sub>. The antibacterial activity of the ligand and its bismuth(III) complex on *S. pombe* was determined by microcalorimetry. The biothermokinetic equation was established according to the measured power–time curves. The quantitative relationships between the thermokinetic parameters such as the growth rate constant (*k*), generation time (*t*<sub>G</sub>) and inhibition ratio (*I*) and with the concentration of the ligand and its bismuth(III) complex were obtained. Furthermore, we further investigated the action target of bismuth(III) complex on BSA by the molecular docking simulation method. As a basic research, one of the purposes of this study is to explore the possibility of microcalorimetric method to predict and evaluate the bioactivity of drugs. On the other hand, it will provide a basis for further study of *N*-alkylation Schiff base and its bismuth compounds.

## Experimental

### Reagents

*o*-Vanillin (VAN) (C<sub>8</sub>H<sub>8</sub>O<sub>3</sub>, 99.0%), pyridine-2,6-dicarboxamide (PCA) (C<sub>7</sub>H<sub>7</sub>N<sub>3</sub>O<sub>2</sub>, 99.0%) and ethanol (EtOH, 99.5%) were purchased from the Sinopharm Chemical Reagent Co., Ltd. (Shanghai, China); dimethylsulfoxide (DMSO, > 99.5%) and *N,N*-dimethyl formamide (DMF, > 99.5%) were bought from Tianjin Guangfu Chemical Research Institute (Tianjin, China); bismuth chloride (BiCl<sub>3</sub>, 99%) was obtained from Tianjin Jingke Chemical Research Institutes (Tianjin, China). All other chemicals including sodium chloride (NaCl, 99.5%), silver nitrate (AgNO<sub>3</sub>, 99.8%) and ethylenediamine tetraacetic acid (EDTA, 99.0%) were purchased from the Sinopharm Chemical Reagent Co., Ltd. (Shanghai, China).

### Cell lines and culture conditions

*S. pombe* (ACCC 20,047) was provided by Beijing Century Aoke Biological Technology Co., Ltd. YES medium (per dm<sup>3</sup>) consisted of yeast (5.000 g), glucose (30.000 g), *L*-leu (0.225 g), *L*-lys (0.225 g), *L*-his (0.225 g), adenine (0.225 g) and uracil (0.225 g). The inoculum medium was sterilized at 120 °C for 30 min in an autoclave. The water used in this work was double-distilled. All chemicals and reagents were used as received without further purification.

### Instrumentation and measurement

Bioactivity was determined by a bio-microcalorimeter (TAM air 3116–2/3239, Switzerland); CY-CR100C-S vertical microwave microreactor (Hunan Changyi Microwave Technology Co., Ltd.) was used to assist the direct condensation *N*-alkylation reaction. Molecular weights of the ligand and its bismuth(III) complex were determined using a LCQ Fleet Ion Trap Mass Spectrometer (Thermo Fisher). FT-IR spectra (400–4000 cm<sup>-1</sup>) were measured using a Thermo Nicolet Avatar 360 Fourier transform IR spectrometer with a KBr pellet. <sup>1</sup>H NMR spectra were recorded on a Bruker 400 MHz advance nuclear magnetic resonance spectrometer with DMSO-*d*<sub>6</sub> as solvent and trimethylsilicane (TMS) as internal standard. The elemental analysis of C, H and N was carried out on a PerkinElmer 2400 elemental analyzer. The content of Bi<sup>3+</sup> in bismuth(III) complex was determined by the EDTA titration and Optima 8300 ICP-OES, respectively. The content of Cl<sup>-</sup> in bismuth(III) complex was determined by Mohr method. All absorption spectra were measured by a Hitachi U-3010 UV–Vis spectrophotometer. The purity of the ligand and its bismuth(III) complex was determined by L-7000 HPLC (Hitachi, Japan). Thermal properties of bismuth(III) complex were determined by a Shimadzu DTG-60 thermogravimetric/differential thermal analyzer (TG/DSC) in flowing air with a heating rate of 10 °C min<sup>-1</sup> between 25 °C and 1450 °C. The molar conductance was determined by a DDS-12DW conductivity meter (Shanghai Lida Instrument Factory, China).

### Synthesis of the ligand

A mass of 4 mmol (about 0.6 g, slightly excess) of powdered VAN was placed in a conical bottle with grinding plug. The conical bottle was placed in a water bath with constant temperature of 60 °C to make VAN melt into bright yellow liquid. Then, a mass of 2 mmol (about 0.3 g) of powdered PCA was added to the melted VAN liquid and stirred evenly, the mixture was yellow and sticky liquid. Subsequently, the mixture was irradiated in a 700 W microwave reactor for

5 min. After taking out and cooling to room temperature, the black-brown solid was ground into powder. After that, DMF was slowly dropped into the beaker containing black powder and stir until the powder was completely dissolved. Bright yellow solid was precipitated out when slightly excess anhydrous ethanol was added into the above solution, and was left to settle for 3 h. Finally, the bright-yellow product was obtained by filtration and washed with a small amount of anhydrous ethanol several times. The product was put into a drying box at 100 °C for 24 h and kept until the mass of the product became constant. The yield was 79%, and the purity was 98.10%. The synthetic scheme of the ligand is depicted in Fig. 1.

### Synthesis of bismuth(III) complex

A mass of 1 mmol of the ligand was placed into a three-neck flask, and then, 5 cm<sup>3</sup> DMF was added with stirring to dissolve it completely (solution A). A mass of 1 mmol of BiCl<sub>3</sub> (slightly excess) was placed into a conical bottle; added 5 cm<sup>3</sup> of DMF by stir to dissolve it completely (solution B). At 60 °C, solution B was added slowly into solution A, and refluxed, heated and stirred for 8 h. As the reaction proceeded, the color of the mixture became brown–red, and an appropriate amount of anhydrous ethanol was added to precipitate the brown–red solid, which was left to settle for 12 h. The brown–red solid was obtained by filtration and washed with a small amount of anhydrous ethanol several times. The product was put in a drying box at 100 °C for 24 h and kept until its mass became constant. The yield of the product was 80%, and its purity was 99.15%. The synthetic scheme of bismuth(III) complex is depicted in Fig. 2.

### Determination of bioactivity of the ligand and its bismuth(III) complex on growth metabolism of *S. pombe*

The bioactivity of the ligand and its bismuth(III) complex on growth metabolism of *S. pombe* was evaluated using ampoule method on a bio-microcalorimeter at 32 °C. The principle and structure of the instrument were elucidated in literature [23]. Once the bio-microcalorimeter reached a stable baseline, 5 cm<sup>3</sup> YES culture medium containing the suspensions of *S. pombe* at the cell density of 1 × 10<sup>6</sup> colony-forming units in each milliliter (CFU cm<sup>-3</sup>) was added to sterilized 20 cm<sup>3</sup> glass ampoules. The ligand and its bismuth(III) complex were injected into the bacterial suspension at different concentrations. Then, all sealed ampoules were shaken up gently and put into the measuring channels. Before the power–time curves were recorded, there was about 30 min for pre-incubation. All signals reflecting thermokinetic information were collected by a computer in a real-time manner.

### Interaction of bismuth(III) complex with BSA

To preliminarily reveal the action mechanism of bismuth(III) complex on *S. pombe* cells, the binding sites of bismuth(III) complex on BSA were investigated by molecular simulation docking using AutoDock Vina software. BSA proteins used for molecular docking were downloaded from PDB database (PDB ID: 4F5S) by MOE(version 2010) software, and to remove water and ligand molecules and retain a chain. Then, the amber 99 force field was added to the protein, and 3D protonation was performed. The structure of the bismuth(III) complex was constructed by Chemdraw

**Fig. 1** Synthetic scheme of the ligand

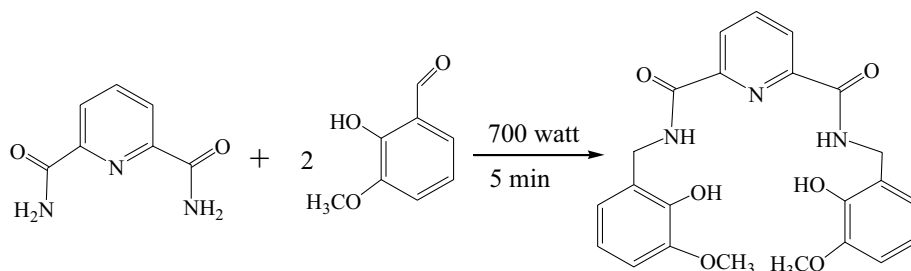
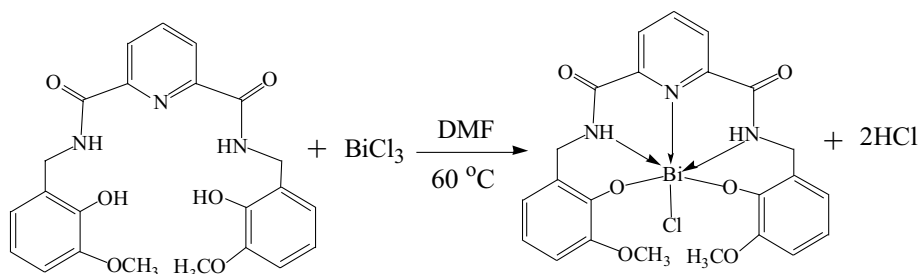


**Fig. 2** Synthetic scheme of bismuth(III) complex



software, and its energy optimization was carried out by MMFF94x force field in MOE. Molecular docking binding mode of bismuth(III) complex with BSA was studied by MOE docking. The possible binding sites were searched by Site Finder algorithm systematically in the BSA to find a total of 40 possible binding pockets. The 40 binding pockets were scored, and the firstly, 20 pockets were screened out as potential pockets for molecular docking; then, 20 docking conformations were selected in each potential pocket for scoring, and the conformation of highest scoring was selected as the best conformation for each pocket. Then, these 20 pockets were ranked according to the score of the best conformation in each pocket, and the highest scoring pocket might be the best binding site of bismuth(III) complex in BSA.

## Results and discussion

### Physical properties of the ligand and its bismuth(III) complex

The ligand and its bismuth(III) complex were bright yellow and brown–red powder, respectively. Both the ligand and its bismuth(III) complex were very easy to dissolve in DMF and DMSO, but difficult to dissolve in methanol, ethanol and acetone, as well as water. The molar conductivities of solution (0.0010 mol dm<sup>-3</sup>) of the ligand and its bismuth(III) complex were determined using DMSO as solvent to be 5.49 and 36.50 S cm<sup>2</sup> mol<sup>-1</sup> at 25 °C, respectively, which showed that they were all non-electrolytes. The melting point of the ligand and its bismuth(III) complex was measured to be 235 ± 1 °C and 264 ± 1 °C by using binocular stereo micro melting point instrument, respectively.

### Elemental and chemical analysis

The measured values (theoretical value) for the elemental analysis of the ligand were as follows: C, 64.44% (64.77%); H, 5.27% (5.02%); N, 9.15% (9.11%). The chemical composition of the complex was determined by elemental analysis for C, H and N, by EDTA titration for Bi<sup>3+</sup> and by AgNO<sub>3</sub> titration for Cl<sup>-</sup>. The found values (theoretical values) for the elemental analysis and chemical analysis of bismuth(III) complex were as follows: C, 42.25% (42.66%); H, 3.09% (3.01%); N, 6.12% (5.97%); Bi, 29.39% (29.69%); Cl, 5.13% (5.04%).

### <sup>1</sup>HNMR and ESI–MS analysis

The <sup>1</sup>HNMR (400 MHz, DMSO-*d*<sub>6</sub>) spectrum and ESI–MS of the ligand were as follows: 10.30(d, 2H, OH), 8.91(d, 2H, NH), 8.22–6.84(m, 9H, Ar–H), 3.74(d, 4H, CH), 3.37(s,

6H, OCH<sub>3</sub>). ESI–MS, (*m/z*): [*M* + H]<sup>+</sup> = 437.2 (Calcd. *M* = 436.2).

The <sup>1</sup>HNMR (400 MHz, DMSO-*d*<sub>6</sub>) spectrum and ESI–MS of bismuth(III) complex were as follows: 8.91(d, 2H, NH), 8.22–7.75(m, 9H, Ar–H), 3.80(d, 4H, CH), 3.40(s, 6H, OCH<sub>3</sub>). ESI–MS, (*m/z*): [*M* + H]<sup>+</sup> = 679.4 and [*M* + Na]<sup>+</sup> = 701.5 (Calcd. *M* = 678.4).

### UV spectra

The UV spectra of the DMSO solution (0.0010 mol dm<sup>-3</sup>) of the ligand and its bismuth(III) complex were determined, which are shown in Fig. 3. It could be seen that the *n*– $\pi^*$  absorption band of the ligand at 340 nm was formed by the coupling of the solitary pair electrons on the *p* orbital of the nitrogen atom in the C–N–C group with the large  $\pi$  bond of the pyridine ring. Moreover, another strong absorption peak at 283 nm was formed by the large  $\pi$ – $\pi^*$  bond of benzene ring conjugation. A larger conjugated system was formed than the ligand when the ligand was coordinated with Bi<sup>3+</sup> ions,  $\pi$ – $\pi^*$  absorption band red-shifts to 306 nm and *n*– $\pi^*$  absorption band blue-shifts to 323 nm and stronger. Finally, this two absorption bands were superimposed into a wide and strong absorption peak.

### IR spectra

The IR spectra of the ligand and its bismuth(III) complex are presented in Fig. 4. From Fig. 4, after the complex was formed, the sharp absorption peak of Ph–OH of the ligand at 3405 cm<sup>-1</sup> was disappeared, which indicated that the phenolic hydroxyl group Ph–O was involved in the coordination. This result has been confirmed by <sup>1</sup>HNMR of the ligand and its bismuth(III) complex. Moreover, compared with the

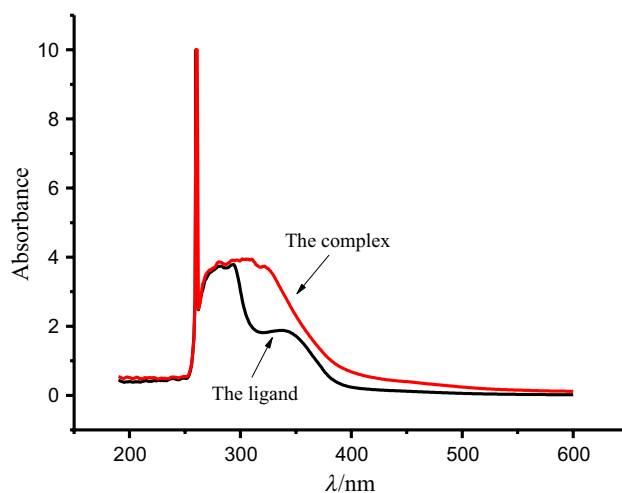
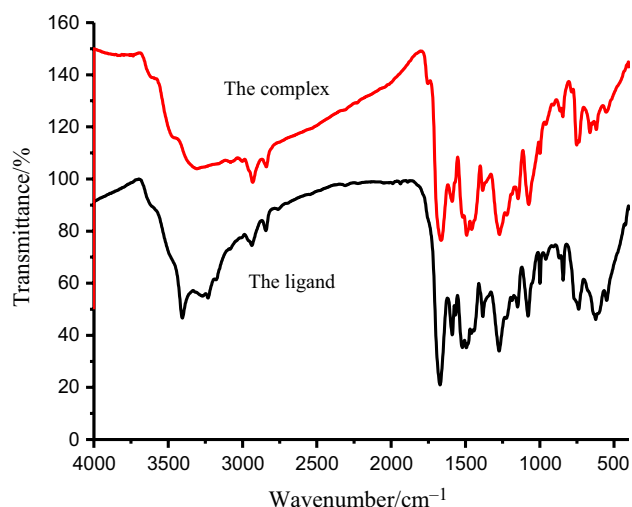


Fig. 3 UV spectra of the ligand and its bismuth(III) complex



**Fig. 4** IR spectra of the ligand and its bismuth(III) complex

ligand the absorption peak (N–H) at  $3232\text{ cm}^{-1}$  red-shifted to  $3307\text{ cm}^{-1}$ , the two absorption peaks (C–N) at  $1383$  and  $1269\text{ cm}^{-1}$  red-shifted to  $1389$  and  $1274\text{ cm}^{-1}$ , indicating that the C–N took part in coordination. The absorption peak of pyridine-N at  $1494\text{ cm}^{-1}$  was split into bi-peak  $1492\text{ cm}^{-1}$  and  $1458\text{ cm}^{-1}$ , indicated that pyridine-N was coordinated with bismuth ion. In low wavelength range, the absorption peaks (C–O) at  $1079\text{ cm}^{-1}$  was blue-shifted to  $1074\text{ cm}^{-1}$ , and single peak (C–N) at  $618\text{ cm}^{-1}$  was split into bi-peak  $660\text{ cm}^{-1}$  and  $615\text{ cm}^{-1}$  compared with the ligand, indicated that the sign of O–Bi<sup>3+</sup> and N–Bi<sup>3+</sup> bond was formed, further confirming that N and O atoms were coordinated with Bi<sup>3+</sup>.

### Thermal properties of bismuth(III) complex

The TG-DSC of the complex was determined in air atmosphere at a heating rate of  $10\text{ °C/min}$  in the range  $25\text{ °C}$  to  $1450\text{ °C}$ , which is shown in Fig. 5. As shown in Fig. 5, there was no mass loss from  $50$  to  $200\text{ °C}$ , which indicated that the complex has no crystal water. The thermal decomposition process of the complex was divided into two steps. In the first step, it had a strong endothermic peak in the range  $230\text{ °C}$  to  $380\text{ °C}$  with a mass loss of  $50.1\%$ , which was close to the theoretical value ( $49.7\%$ ) due to the loss of  $1\text{ mol}$  of Cl and  $2\text{ mol}$  of  $\text{C}_8\text{H}_9\text{O}_2\text{N}$  (VAN is the main structure). In the second step, it had a weak endothermic peak in the range  $380\text{ °C}$  to  $516\text{ °C}$  with a mass loss of  $20.2\%$ , which corresponds to the loss of  $1\text{ mol}$  of  $\text{C}_7\text{H}_3\text{O}_2\text{N}$  (PCA is the main structure) (theoretical value is  $19.6\%$ ) (The loss involves two processes. One is the carbon–nitrogen bond breaking, which involves endothermic process. The other is the bismuth–oxygen bond forming, which involves exothermic process. Bond formation and fracture occur almost simultaneously, and the corresponding endothermic and exothermic process offsets

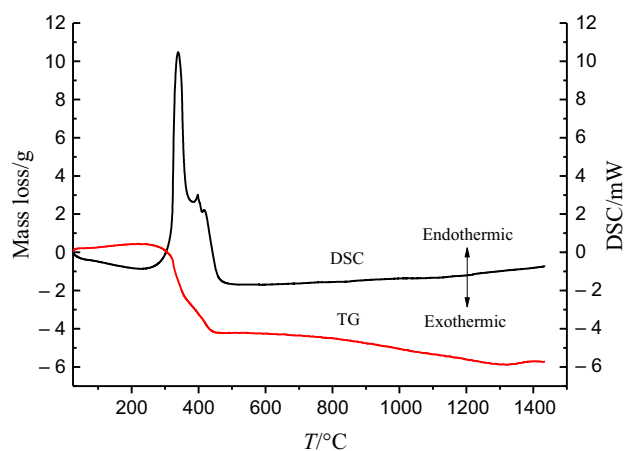


**Fig. 5** TG-DSC diagram of bismuth(III) complex

each other partially. Thus, it exhibits a weak endothermic peak.). The final product of complete decomposition of the complex was  $\text{Bi}_2\text{O}_3$  by ICP analysis. The molecular formula of the complex is  $\text{Bi}(\text{C}_{23}\text{H}_{21}\text{O}_6\text{N}_3)\text{Cl}$  by experimental and theoretical calculated results, whose mechanism of thermal decomposition was as follows:



It is worth mentioning that the melting point of bismuth (III) complex was measured to be  $264 \pm 1\text{ °C}$  by using binocular stereo micro melting point instrument, but on the DSC curve could not be observed any sign of melting. It may be that the melting temperature of the complex is very close to its decomposition temperature, resulting in the endothermic peak of melting and the endothermic peak of decomposition overlaps each other, so the endothermic peak of complex melting is not obvious on the curve.

To sum up, it was finally inferred that the compositions of the ligand and its bismuth(III) complex were  $\text{C}_{23}\text{H}_{23}\text{N}_3\text{O}_6$  and  $\text{Bi}(\text{C}_{23}\text{H}_{21}\text{O}_6\text{N}_3)\text{Cl}$ , respectively. Their possible chemical structures are depicted in Fig. 6.

### Microcalorimetry

#### Power–time curves

When the suspensions of *S. pombe* are introduced into the ampoules with YES culture medium, the power–time curve of *S. pombe* growth of blank control is plotted in Fig. 7a. As depicted in Fig. 7a, the observable growth curve of *S. pombe* consisted of four phases [the lag phase (AB), the exponential phase (BC), the stationary phase (CD) and the decline phase (DE)]. As the suspensions of *S. pombe* are added to the ampoules with different concentrations of the ligand and

**Fig. 6** Chemical structure of the ligand **(a)** and its bismuth(III) complex **(b)**

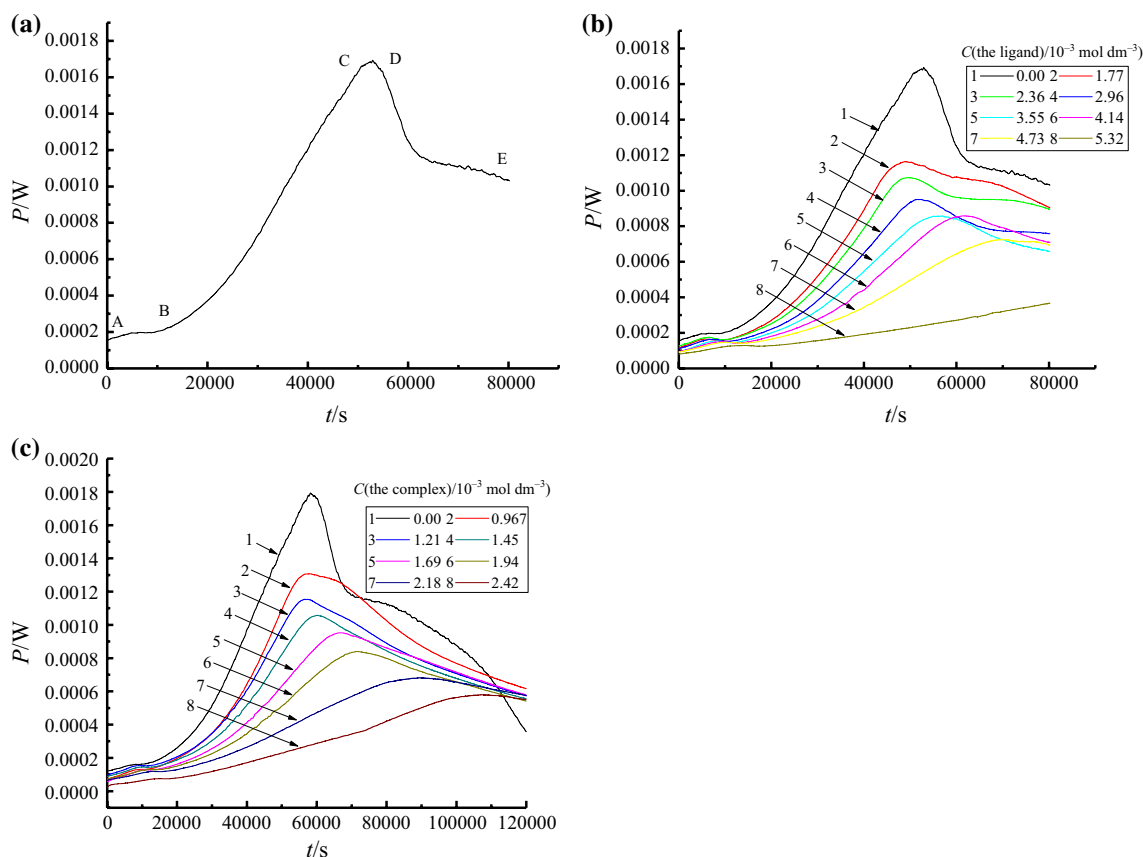
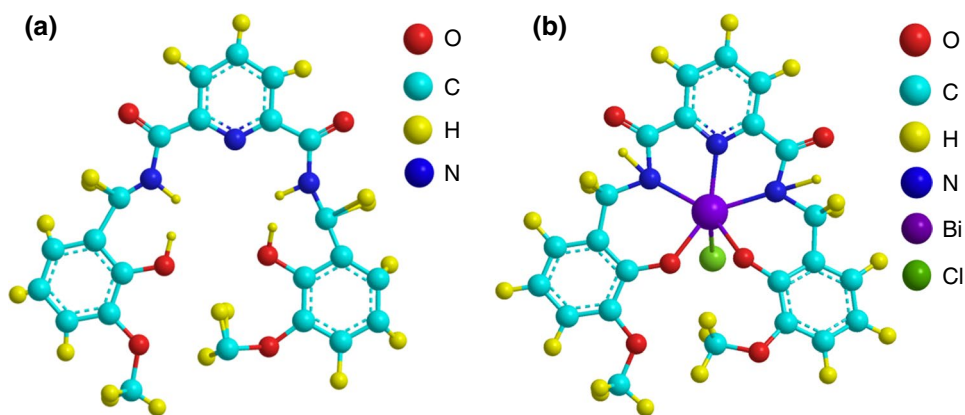


**Fig. 7** Power–time curves of the growth of *S. pombe* affected by **a** blank control, **b** the ligand and **c** its bismuth(III) complex at 32 °C

its bismuth(III) complex, the shapes of  $P-t$  curves were also changed (Fig. 7b, c). The curves in Fig. 7 illustrated that the height, peak time and shape of each experimental group were obviously different from the blank control group.

### Biothermokinetics

In the exponential growth phase, the biothermokinetic equation of growth metabolic of *S. pombe* could be

established by simulating the exponential equation, as shown in Eq. 1 [24]:

$$n_t = n_0 \exp[k(t - t_0)] \quad (1)$$

where  $t_0$  was the initial time of logarithmic period,  $t$  was any time of logarithmic period.  $n_t$  and  $n_0$  represented the bacterial number at time  $t$  and  $t_0$ , respectively. If the power

produced by every bacterium is  $w$ , then we can obtain the following equation

$$n_t w = n_0 w \exp[k(t - t_0)] \quad (2)$$

Making  $p_t = n_t w$ ,  $p_0 = n_0 w$ , then Eq. (2) can change to

$$p_t = p_0 \exp[k(t - t_0)] \quad (3)$$

or

$$\ln p_t = \ln p_0 - kt_0 + kt$$

or

$$\ln p_t = A + kt \quad (4)$$

where  $p_t$  was the power output at time  $t$  and  $k$  was growth rate constant for *S. pombe* at specified conditions. Then,  $\ln p_t$  against  $t$  was plotted and fitted linearly to obtain its linear equation. The growth rate constant  $k$  was obtained according to slope of linear equation. The values of  $k$  are listed in Table 1.

#### Quantitative relationship between $k$ and $c$

The  $k$  values in Table 1 revealed that Schiff base and its bismuth(III) complex had both potent antibacterial activity against *S. pombe* and the complex displayed stronger inhibition than the ligand. The quantitative relationship between  $k$  and  $c$  is demonstrated in Fig. 8.

The  $k$  of *S. pombe* decreased with the increasing concentration ( $c$ ). This may be due to *S. pombe* cells being suppressed or killed by the tested drug, which reduces metabolic

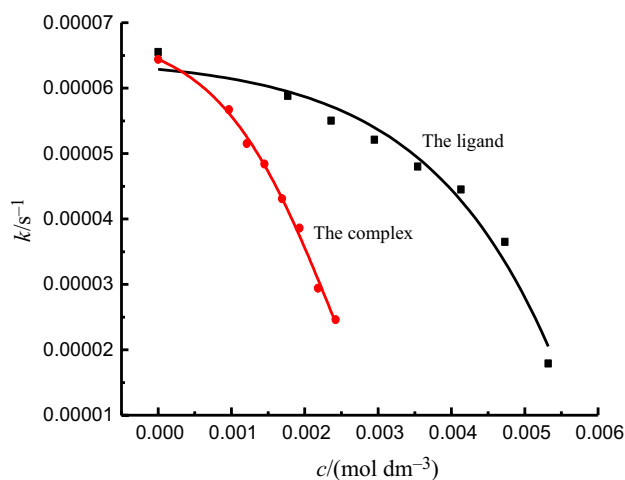


**Fig. 8** Relationships between the growth rate constant ( $k$ ) of *S. pombe* and concentration ( $c$ ) of the ligand and its bismuth(III) complex

thermal power. The  $k$ - $c$  equations could be described as below:

$$k_{\text{the ligand}} = -5.4 \times 10^{-4} + 6.0 \times 10^{-4} / [1 + e^{625(c-0.00938)}] \quad (5)$$

$(0.00 \text{ mol dm}^{-3} \leq c \leq 5.32 \times 10^{-3} \text{ mol dm}^{-3})$

$$k_{\text{the complex}} = -7.0 \times 10^{-4} + 9.0 \times 10^{-4} / [1 + e^{1250(c-0.00243)}] \quad (6)$$

$(0.00 \text{ mol dm}^{-3} \leq c \leq 2.42 \times 10^{-3} \text{ mol dm}^{-3})$

**Table 1** Thermokinetic parameters of the growth of *S. pombe* treated by different concentrations of the ligand and its bismuth(III) complex at 32 °C

Drugs	$c^a/\text{mol dm}^{-3}$	$k^b/\text{s}^{-1}$	$t_G^c/\text{s}$	$I^d$	$IC_{50}^e/\text{mol dm}^{-3}$
The ligand	0.00	$6.55 \times 10^{-5} \pm 3.5 \times 10^{-8f}$	$1.06 \times 10^4$	0.00	$4.63 \times 10^{-3}$
	$1.77 \times 10^{-3}$	$5.88 \times 10^{-5} \pm 3.5 \times 10^{-8}$	$1.18 \times 10^4$	10.23	
	$2.36 \times 10^{-3}$	$5.50 \times 10^{-5} \pm 3.1 \times 10^{-8}$	$1.26 \times 10^4$	16.03	
	$2.96 \times 10^{-3}$	$5.21 \times 10^{-5} \pm 2.9 \times 10^{-8}$	$1.33 \times 10^4$	20.46	
	$3.55 \times 10^{-3}$	$4.80 \times 10^{-5} \pm 2.9 \times 10^{-8}$	$1.44 \times 10^4$	26.72	
	$4.14 \times 10^{-3}$	$4.45 \times 10^{-5} \pm 1.9 \times 10^{-8}$	$1.56 \times 10^4$	32.06	
	$4.73 \times 10^{-3}$	$3.65 \times 10^{-5} \pm 9.4 \times 10^{-9}$	$1.90 \times 10^4$	44.28	
	$5.32 \times 10^{-3}$	$1.79 \times 10^{-5} \pm 1.0 \times 10^{-8}$	$3.87 \times 10^4$	72.67	
The complex	0.00	$6.44 \times 10^{-5} \pm 4.0 \times 10^{-8}$	$1.08 \times 10^4$	0.00	$2.10 \times 10^{-3}$
	$9.68 \times 10^{-4}$	$5.67 \times 10^{-5} \pm 3.2 \times 10^{-8}$	$1.22 \times 10^4$	10.56	
	$1.21 \times 10^{-3}$	$5.15 \times 10^{-5} \pm 3.4 \times 10^{-8}$	$1.35 \times 10^4$	20.03	
	$1.45 \times 10^{-3}$	$4.84 \times 10^{-5} \pm 3.2 \times 10^{-8}$	$1.43 \times 10^4$	24.85	
	$1.69 \times 10^{-3}$	$4.31 \times 10^{-5} \pm 3.6 \times 10^{-8}$	$1.61 \times 10^4$	33.08	
	$1.94 \times 10^{-3}$	$3.86 \times 10^{-5} \pm 3.2 \times 10^{-8}$	$1.80 \times 10^4$	40.06	
	$2.18 \times 10^{-3}$	$2.94 \times 10^{-5} \pm 4.4 \times 10^{-8}$	$2.36 \times 10^4$	54.35	
	$2.42 \times 10^{-3}$	$2.46 \times 10^{-5} \pm 4.0 \times 10^{-8}$	$2.82 \times 10^4$	61.80	

<sup>a</sup>The concentration; <sup>b</sup>The growth rate constant of *S. pombe*; <sup>c</sup>The generation time; <sup>d</sup>The inhibition ratio; <sup>e</sup>The half inhibition concentration; <sup>f</sup>Mean  $\pm$  SD,  $n = 3$

### Quantitative relationship between $t_G$ and $c$

Because the biothermokinetic Eq. (4) was very similar to the indefinite integral relation of rate equation of the first order reaction, the mathematical expression of generation time ( $t_G$ ) of *S. pombe* could be defined by simulating the relationship between the half-life of the first-order reaction and the rate constant of the reaction (see Eq. 7):

$$t_G = \ln 2/k \quad (7)$$

where  $t_G$  was the generation time and  $k$  was growth rate constant of *S. pombe*. The  $t_G$  of *S. pombe* were calculated at different concentration of the ligand and its bismuth(III) complex. As summarized in Table 1, the  $t_G$  was longer than that of blank control. With increasing concentration of the ligand and its bismuth(III) complex, the  $t_G$  prolonged. It is because that, after the treatment with the tested drugs, there was a partial inhibition of *S. pombe* and other survivor maintained growth and metabolized at a lower rate.

The  $t_G$ - $c$  curves were drawn for the generation time ( $t_G$ ) and the concentration ( $c$ ) of the ligand and its bismuth(III) complex (Fig. 9).

The correlation between  $t_G$  and  $c$  could be formulated according to following equations:

$$t_{G(\text{the ligand})} = 11333.274 + 5.367 \times 10^{-2} / [4(c - 0.00597)^2 + 2.60 \times 10^{-7}] \quad (8)$$

(0.00 mol dm<sup>-3</sup> ≤  $c$  ≤ 5.32 × 10<sup>-3</sup> mol dm<sup>-3</sup>)

$$t_{G(\text{the complex})} = 10058.944 + 2.721 \times 10^{-2} / [4(c - 0.0026)^2 + 1.37 \times 10^{-6}] \quad (9)$$

(0.00 mol dm<sup>-3</sup> ≤  $c$  ≤ 2.42 × 10<sup>-3</sup> mol dm<sup>-3</sup>)

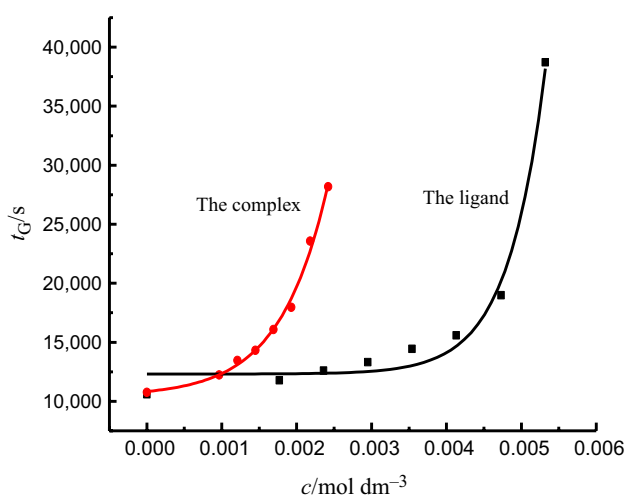


**Fig. 9** Relationships between the generation time ( $t_G$ ) of *S. pombe* and concentration ( $c$ ) of the ligand and its bismuth(III) complex

### Inhibition ratio ( $I$ ) and half inhibition concentration ( $IC_{50}$ )

The inhibition ratio ( $I$ ) of the growth metabolism of *S. pombe* treated by the ligand and its bismuth(III) complex could be defined as follows:

$$I = (k_0 - k_c) / k_0 \times 100\% \quad (10)$$

where  $k_0$  and  $k_c$  are the growth rate constants of *S. pombe* without and with the tested drugs, respectively. When the inhibition ratio ( $I$ ) was 50%, the corresponding concentration of inhibitor was called as the half inhibition concentration  $IC_{50}$ . The values of  $I$  and  $IC_{50}$  are shown in Table 1.

The inhibition ratio ( $I$ ) and concentration ( $c$ ) of the ligand and its bismuth(III) complex are plotted in Fig. 10.

From the data in Table 1 and the plot in Fig. 10, we could see that the inhibition ratio ( $I$ ) was both increased with the increasing of concentration ( $c$ ) of the ligand and its bismuth(III) complex, indicated that the growth of *S. pombe* was both inhibited by two tested drugs and the inhibitory effect of the complex was stronger than that of the ligand. The quantitative relationship between inhibition ratio ( $I$ ) and concentration ( $c$ ) by nonlinear fitting could be described in Eqs. (11) and (12):

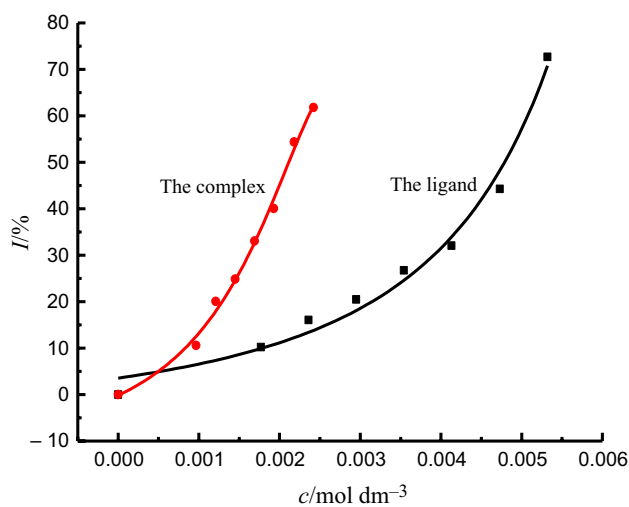


**Fig. 10** Relationships between inhibition ratio ( $I$ ) of *S. pombe* and concentrations ( $c$ ) of the ligand and its bismuth(III) complex



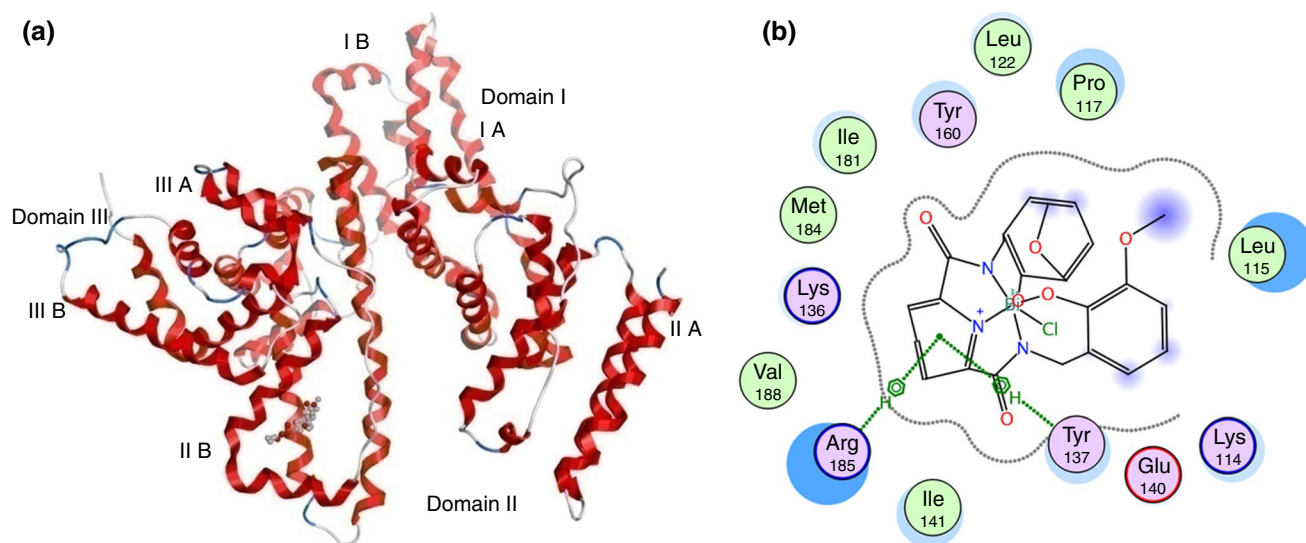


**Fig. 11** **a** The docking conformation of bismuth(III) complex-BSA complex with lowest energy and **b** the amino acid residues of surround bismuth(III) complex

$$I_{(\text{the ligand})} = 2.75 \times 10^{-3} / [4(c - 0.00811)^2 + 4.37 \times 10^{-6}] - 6.7686$$

$$(0.00 \text{ mol dm}^{-3} \leq c \leq 5.32 \times 10^{-3} \text{ mol dm}^{-3}) \quad (11)$$

$$I_{(\text{the complex})} = 5.41 \times 10^{-4} / [4(c - 0.00281)^2 + 6.45 \times 10^{-6}] - 14.4142$$

$$(0.00 \text{ mol dm}^{-3} \leq c \leq 2.42 \times 10^{-3} \text{ mol dm}^{-3}) \quad (12)$$

Meanwhile, the half inhibition concentration ( $IC_{50}$ ) of the ligand and its bismuth(III) complex was obtained to be  $4.63 \times 10^{-3} \text{ mol dm}^{-3}$  and  $2.10 \times 10^{-3} \text{ mol dm}^{-3}$ , respectively. The results have shown that the bioactivity of the complex was greater than that of the ligand. Therefore, we believed that the bioactivity of the complex was not only related to the structure of the ligand, but more important depended on the property of bismuth(III) ion.

### Action target of bismuth(III) complex on bovine serum albumin (BSA)

Action target of BSA interaction with bismuth(III) complex was studied by molecular docking as shown in Fig. 11.

Figure 11a illustrates that bismuth(III) complex bound at the hydrophobic cavity of the substructure domain IIB of BSA and was the best conformation of bismuth (III) complex-BSA complex with lowest energy. Figure 11b shows that the amino acid residues interacting with bismuth(III) complex were: Leu115, Pro117, Leu122, Tyr160, Ile181, Met184, Lys136, Val188, Arg185, Ile141, Tyr137, Glu140 and Lys114. The Trp137 and Arg185 interacted with

bismuth(III) complex through hydrogen bonds, while the remaining amino acid residues interacted with the complex via hydrophobic and van der Waals; these were consistent with the literatures [25, 26].

### Conclusions

In this work, we described the synthesis of a new *N*-alkylation Schiff base and its bismuth(III) complex for the first time, and their compositions and structures were characterized using various physicochemical detection methods. Moreover, the biothermokinetic and bioactivity of Schiff base and its bismuth(III) complex on growth metabolism of *S. pombe* were studied. Some thermokinetic parameters ( $k$ ,  $t_G$  and  $I$ ) and their quantitative relationship with concentration were investigated. Finding that two compounds had both inhibition effects on *S. pombe* cells and the inhibitory effect of the complex was stronger than that of the ligand. Besides the action target of bismuth(III) complex on BSA was investigated by molecular docking simulation method, it was found that they bind mainly to amino residues in the subdomain IIB of the hydrophobic cavity of BSA.

**Acknowledgements** The authors thank the National Natural Science Foundation of China (No. 21273190), the Hunan Provincial Natural Science Foundation of China (No. 2017JJ2240), the Project of Scientific Research of Hunan Provincial Education Department (No.18B499, No.17C1472 and No.15A175) and the National Students' Project for Innovation and Entrepreneurship Training Program (No.201910545038) for financial support.

## Declarations

**Conflict of interest** The authors claim that there are no conflicts of interest.

## References

- Backes GL, Neumann DM, Jursic BS. Synthesis and antifungal activity of substituted salicylaldehydehydrazones, hydrazides and sulfohydrazides. *Bioorg Med Chem*. 2014;22:4629–36.
- Friedman M, Henika PR, Mandrell RE. Antibacterial activities of phenolic benzaldehydes and benzoic acids against *Campylobacter jejuni*, *Escherichia coli*, *Listeria monocytogenes*, and *Salmonella enteric*. *J Food Prot*. 2003;66:1811–21.
- Li QG, Zhang H, Li X, Wang B, Hu JL, Yao FH, Yang DJ, Xiao SX, Ye LJ. Synthesis of thioproline salicylic acid samarium complex and microcalorimetric study on effects of the complex on the growth metabolism of *S. pombe* cells. *Chinese J Chem*. 2011;29:2285–92.
- Katsura Y, Tomishi T, Inoue Y, Sakane K, Matsumoto Y, Morinaga C, Ishikawa H, Takasugi H. Anti-*Helicobacter pylori* agents. 4. 2-(substituted guanidino)-4-phenylthiazoles and some structurally rigid derivatives. *J Med Chem*. 2000;43:3315–21.
- Ando R, Kawamura M, Chiba N. 3-(arylacetylamino)-*N*-methylbenzamides: a novel class of selective anti-*Helicobacter pylori* agents. *J Med Chem*. 2001;44:4468–74.
- Al-Omar MA, Amr AEE. Synthesis of some new pyridine-2,6-carboxamide-derived Schiff bases as potential antimicrobial agents. *Molecules*. 2010;15:4711–21.
- Sun HZ, Li HY, Sadler PJ. The biological and medicinal chemistry of bismuth. *Chem Ber/Recuei*. 1997;130:669–81.
- Briand GG, Burford N. Bismuth compounds and preparations with biological or medicinal relevance. *Chem Rev*. 1999;99:2601–57.
- Kotani T, Nagai D, Asahi K, Suzuki H, Yamao F, Kataoka N, Yagura T. Antibacterial properties of some cyclic organobismuth(III) compounds. *Antimicrob Agents Ch*. 2005;49:2729–34.
- Islam A, Rodrigues BL, Marzano IM, Perreira-Maia EC, Ditz D, Lopes MTP, Ishfaq M, Frezard F, Demicheli C. Cytotoxicity and apoptotic activity of novel organo-bismuth(V) and organoantimony(V) complexes in different cancer cell lines. *Eur J Med Chem*. 2016;109:254–67.
- Li X, Li CH, Jiang JH, Gu HW, Wei DL, Ye LJ, Hu JL, Xiao SX, Guo DC, Li X, Zhang H, Li QG. Synthesis and microcalorimetric determination of the bioactivities of a new Schiff base and its bismuth(III) complex derived from *o*-vanillin and 2,6-pyridinediamine. *J Therm Anal Calorim*. 2017;127:1767–76.
- Andrews PC, Ferrero RL, Junk PC, Kumar I, Luu Q, Nguyen K, Taylor JW. Bismuth(III) complexes derived from non-steroidal anti-inflammatory drugs and their activity against *Helicobacter pylori*. *Dalton Trans*. 2010;39:2861–8.
- Andrews PC, Ferrero RL, Forsyth CM, Junk PC, Maclellan JG, Peiris RM. Bismuth(III) saccharinate and thiosaccharinate complexes and the effect of ligand substitution on their activity against *Helicobacter*. *Organometallics*. 2011;30:6283–91.
- Kowalik M, Masternak J, Barszcz B. Recent research trends on bismuth compounds in cancer chemo and radiotherapy. *Curr Med Chem*. 2019;26:729–59.
- Yang N, Sun HZ. Biocoordination chemistry of bismuth: recent advances. *Coordin Chem Rev*. 2007;251:2354–66.
- Murafuji T, Miyoshi Y, Ishibashi M, Rahman AFM, Sugihara Y, Miyakawa I, Uno H. Antifungal activity of organobismuth compounds against the yeast *Saccharomyces cerevisiae*: structure-activity relationship. *J Inorg Biochem*. 2004;98:547–52.
- Murafuji T, Tomura M, Ishiguro K, Miyakawa I. Activity of antifungal organobismuth(III) compounds derived from alkyl aryl ketones against *S cerevisiae*: comparison with a heterocyclic bismuth scaffold consisting of a diphenyl sulfone. *Molecules*. 2014;19:11077–95.
- Cortes JC, Carnero E, Ishiguro J, Sanchez Y, Durán A, Ribas JC. The novel fission yeast (1,3)beta-D-glucan synthase catalytic subunit Bgs4p is essential during both cytokinesis and polarized growth. *J Cell Sci*. 2005;118:157–74.
- Xie W, Zhou LJ, Xu J, Guo QL, Jiang FL, Liu Y. Advances in biothermochemistry and thermokinetics. *Acta Phys-Chim Sin*. 2020;36:1905051.
- Braissant O, Bachmann A, Bonkat G. Microcalorimetric assays for measuring cell growth and metabolic activity: methodology and applications. *Methods*. 2015;76:27–34.
- Hu XK, Ma Y, Liu ZD, Zhao MX, Dong SM, Yang H, Dai CM. Microcalorimetric evaluation of the effects of three anthraquinone derivatives from Chinese Rhubarb and the synergistic effect of the mixture on *Staphylococcus aureus*. *J Therm Anal Calorim*. 2020;141:739–49.
- Chen C, Qu F, Wang J, Xia XH, Wang JB, Chen Z, Ma X, Wei SZ, Zhang YM, Li JY, Gong M, Wang RL, Liu HH, Yang ZR, Li YG, Zhao YL, Xiao XH. Antibacterial effect of different extracts from *Wikstroemia indica* on *Escherichia coli* based on microcalorimetry coupled with agar dilution method. *J Therm Anal Calorim*. 2016;123:1583–90.
- Li X, Jiang JH, Chen QQ, Xiao SX, Li CH, Gu HW, Zhang H, Hu JL, Yao FH, Li QG. Synthesis of nordihydroguaiaretic acid derivatives and their bioactivities on *S pombe* and K562 cell lines. *Eur J Med Chem*. 2013;62:605–13.
- Xie CL, Tang HK, Song ZH, Qu SS, Liao YT, Liu HS. Microcalorimetric study of bacterial growth. *Thermochim Acta*. 1988;123:33–41.
- Lou YY, Zhou KL, Shi JH, Pan DQ. Characterizing the binding interaction of fungicide boscalid with bovine serum albumin (BSA): a spectroscopic study in combination with molecular docking approach. *J Photoch Photobio B*. 2017;173:589–97.
- Han XL, Lai L, Tian FF, Jiang FL, Xiao Q, Li Y, Yu QLY, Li DW, Wang J, Zhang QM, Zhu BF, Li R, Liu Y. Toxicity of CdTe quantum dots on yeast *saccharomyces cerevisiae*. *Small*. 2012;8:2680–9.

**Publisher's Note** Springer Nature remains neutral with regard to jurisdictional claims in published maps and institutional affiliations.